Involvement of MEK/ERK1/2 and PI3K/Akt Pathways in the Refractory Behavior of GH3B6 Pituitary Tumor Cells to the Inhibitory Effect of TGFβ1

Juan Pablo Petiti, Liliana del Valle Sosa, María Eugenia Sabatino, Alicia Maldré Vaca, Silvina Gutiérrez, Ana Lucía De Paul, and Alicia Inés Torres

Centro de Microscopía Electrónica, Instituto de Investigaciones en Ciencias de la Salud-Consejo Nacional de Investigaciones Científicas y Técnicas and Facultad de Ciencias Médicas, Universidad Nacional de Córdoba, 5000-Córdoba, Argentina

Pituitary tumor cells have a poor response to the growth inhibitory effect of TGFβ1, possibly resulting from the cross talk of TGFβ/Smads signal with other signaling pathways, an undescribed mechanism in these tumoral cells. To address this hypothesis, we investigated whether the mitogen-activated extracellular signal-regulated kinase (MEK)/ERK1/2 and phosphoinositide-3 kinase/protein kinase B (PI3K/Akt) pathways were able to regulate the antimitogenic effect of TGFβ1 on GH3B6 cells. TGFβ1 treatment decreased the cell proliferation and induced an activation of mothers against decapentaplegic homolog 2/3 (Smad2/3), effects that were potentiated by MEK and PI3K inhibitors, thus indicating the existence of a cross talk between TGFβ1/Smad with the MEK/ERK1/2 or PI3K/Akt pathways. In addition, through immunoprecipitation assays, a direct interaction was observed between Smad2/3-ERK1/2 and Smad2/3-Akt, which decreased when the GH3B6 cells were incubated with TGFβ1 in the presence of MEK or PI3K inhibitors, thereby suggesting that the ERK1/2- and Akt-activated states were involved. These Smad2/3-ERK1/2 and Smad2/3-Akt associations were also confirmed by confocal and transmission electron microscopy. These findings indicate that the TGFβ1-antimitogenic effect in GH3B6 cells was attenuated by the MEK/ERK1/2 and PI3K/Akt pathways via modulating Smad2/3 phosphorylation. This molecular mechanism could explain in part the refractory behavior of pituitary tumor cells to the inhibitory effect of TGFβ1. **(*Endocrinology* 156: 534–547, 2015)**

Changes occurring in the balance between the positive and negative regulators that control cellular growth constitute a mechanism by which cells escape from their normal control and become tumoral cells. Among the negative regulators, TGFβ is characterized by its contribution in modulating a wide range of processes, including proliferation, differentiation, embryogenesis, immune regulation, and tissue repair (1, 2). TGFβ is generally considered to be a tumor suppressor, but aberrant TGFβ signaling is associated with the formation and progression of tumors (3).

In the pituitary gland, it has been demonstrated that TGFβ1 is produced and secreted by lactotroph and folliculostellate cells, with it having been shown to be a potent inhibitor of prolactin secretion and cell proliferation of prolactin (PRL) cells (4–6). However, regarding pituitary tumor cells, a poor response has been observed to the growth inhibitory effect of TGFβ1, which was associated with the low expression of TGFβ receptors (7). Furthermore, in prolactinoma induced by estrogen, a decrease of expression of TGFβ receptor proteins and mRNA during tumor development was detected, in

ISSN Print 0013-7227 ISSN Online 1945-7170
Printed in U.S.A.

Received January 24, 2014. Accepted November 10, 2014.
First Published Online November 13, 2014

Abbreviations: BIM, bisindolylmaleimide I; BrdU, bromodeoxyuridine; EGF, epidermal growth factor; EM, electron microscopy; JNK, Jun N-terminal kinase; LY294002, 2-(4-Morpholinyl)-8-phenyl-1(4H)-benzopyran-4-one hydrochloride; MEK, mitogen-activated extracellular signal-regulated kinase; p38, protein kinase of 38 kDa; PD98059, Dimethyl sulfoxide 2-(2-Amino-3-methoxyphenyl)-4H-1-benzopyran-4-one; PI, propidium iodide; PI3K/Akt, phosphoinositide-3 kinase/protein kinase B; PKC, protein kinase C; PRL, prolactin; p-Smad2/3, phospho-Smad2/3; RIA, radioimmunoassay; Smad, mothers against decapentaplegic homolog; TEM, transmission EM; TβRI , TGFβ type I receptor.

agreement with the low levels found in the GH3 pituitary tumor cell line (8).

TGFβ1 signaling is mediated by TGFβ type I receptor (TβRI) and TβRII, which form a heterotetrameric complex located on the plasma membrane consisting of 2 TβRI and 2 TβRII. Upon TGFβ binding, the TβRII receptors phosphorylate the TβRI receptors, resulting in their activation. The activated TβRI receptors then phosphorylate mothers against decapentaplegic homolog (Smad) 2 and Smad3 at the C-terminal serines, which form trimers with Smad4 that translocate into the nucleus, where they regulate the expression of genes that control cell cycle progression (9). TGFβ can also use non-Smad signaling pathways, such as protein kinase of 38 kDa (p38), Jun N-terminal kinase (JNK), and MAPK pathways, to convey its signals (10).

Additional phosphorylation by intracellular protein kinases may regulate the Smads positively or negatively. Related to this, it has been demonstrated that ERK, JNK, and p38 MAPK phosphorylate Smad2/3, thus regulating the stability, activity, and transport of the Smads (11). Another signaling pathway involved in the modulation of TGFβ signaling is phosphoinositide-3 kinase/protein kinase B (PI3K/Akt), which alleviates TGFβ-induced cell cycle arrest in different cell types in response to stimuli (12, 13). These studies have shown the existence of cross talk between the TGFβ/Smad pathways and other signaling that regulates the antiproliferative effect of this growth factor. Moreover, attenuation of the TGFβ/Smad signaling pathway is a mechanism by which different tumoral cells evade the antiproliferative effect of TGFβ1 (14).

The PI3K/Akt and MAPKs pathways are the 2 major signaling pathways responsible for regulating cell growth and proliferation, which are activated by growth factor receptors (15). In human pituitary tumor studies, although the existence of a constitutive increase of the rat sarcoma/ERK and/or PI3K/Akt pathway activities has been reported (16, 17), the molecular mechanisms by which proliferative signaling pathways may contribute to the refractory inhibitory effect of TGFβ/Smads in pituitary tumor cells still remain unknown.

The future identification of intracellular targets that mediate responses to inhibitor signals will increase the understanding of the pathways involved in the pituitary tumor development. In the present study, our objectives were to determine the modulator role of the mitogen-activated extracellular signal-regulated kinase (MEK)/ERK1/2 and PI3K/Akt signaling pathways in the antiproliferative effect of TGFβ/Smad in GH3B6 pituitary tumor cells and to identify the intracellular mediators that may contribute in the response to the TGFβ1 signal. This regulatory mechanism would provide a better understanding of the aberrations responsible for TGFβ1 signal dysfunction in tumorigenesis.

Materials and Methods

Cell culture

The rat GH3B6 lactosomatotroph pituitary adenoma cell line derives from GH3 cells, which secretes high levels of prolactin, is an adequate in vitro prolactinoma model (18, 19). The cells were cultured in Ham's F-12 Nutrient Mixture medium supplemented with 5% fetal calf serum and 12% horse serum (Invitrogen) in an oven with a humidified atmosphere of 5% CO_2 and 95% air at 37°C. All cell culture grade reagents were obtained from Sigma. After 3 days of culture and with a confluence of 70%, the cells were submitted to different experimental protocols.

Cell treatments

Transforming growth factorβ1

TGFβ1 (Sigma) was solubilized in dimethyl sulfoxide before being added to cell media at different concentration (2 or 4 ng/mL) and times (30 min and 7, 16, and 24 h).

Epidermal growth factor (EGF)

Experiments were performed using EGF (Sigma) at a concentration of 10 ng/mL for 30 minutes in serum-free Ham's F-12 Nutrient Mixture medium.

Inhibitors

The inhibitor of mitogen-activated kinase effector kinase Dimethyl sulfoxide 2-(2-Amino-3-methoxyphenyl)-4H-1-benzopyran-4-one (PD98059) (50μM; Calbiochem) (20), the specific PI3K inhibitor 2-(4-Morpholinyl)-8-phenyl-1(4H)-benzopyran-4-one hydrochloride (LY294002) (10μM; Sigma) (21), and the pan-protein kinase C (PKC) inhibitor bisindolylmaleimide I (BIM) (4μM; Sigma) (22) were added separately for 30 minutes before stimulation with TGFβ1 (4 ng/mL) for 30 minutes or 24 h.

At the end of each experimental condition with PD98059 and LY294002, the cells were subjected to Western blotting and cell cycle analyses by flow cytometry. The culture media were collected and stored frozen at −20°C before determining the PRL levels by radioimmunoassay (RIA) in the assays that used BIM and PD98059.

Flow cytometric cell cycle analysis

GH3B6 cells were harvested, washed in PBS, fixed with ethanol 70%, and incubated with ribonuclease A (10 μg/μL, Sigma R5503). This was followed by DNA staining with propidium iodide (50 μg/mL; Sigma P4170) in order to analyze the cellular DNA content. Cell cycle analysis was performed on a Coulter flow cytometer (BD FACS Canto II), with the percentage of cells in the S and G_2/M phase fractions being combined to serve as a proliferative index.

Bromodeoxyuridine incorporation and cell cycle analysis

The analysis of the cell cycle through bromodeoxyuridine (BrdU) incorporation was performed according to Ref. 23 with modifications. Briefly, BrdU (3 mg/mL) was added during the final 30 minutes of the treatments mentioned above. Then, GH3B6 cells were detached with TrypLE Express, washed twice with PBS, and fixed overnight with 70% of ethanol. The DNA was denatured for 15 minutes with 2M hydrochloric acid followed by neutralization with sodium tetraborate solution (0.1M; pH 8.5). After washing, cells were incubated with BrdU monoclonal primary antibody (1:100; GE Healthcare Life Sciences) at 37°C for 20 minutes, followed by incubation with secondary antibody Alexa Fluor 488 (1:1000; Invitrogen) for 1 h at 37°C. Finally, GH3B6 cells were resuspended in propidium iodide (50 μg/mL; Sigma P4170) overnight at 4°C, and RNAse 10 μg/μL was added 30 minutes before running the sample on a flow cytometer (FaCScan; Ortho Diagnostic System). The data analysis was carried out using the FlowJo software (Tree Star, Inc) (for antibodies, see Table 1).

Immunoprecipitation

Protein extract of tumoral pituitary cells (1 mg of protein) were obtained according to previous protocols (24) and then were subjected to immunoprecipitation using specific goat antiserum against phospho-Smad2/3 (p-Smad2/3) (5 μL). The immune complexes were adsorbed and precipitated using Protein G-Sepharose beads (Sigma-Aldrich), washed 3 times with lysis buffer and denatured by boiling for 5 min in the sample buffer. Parallel immunoprecipitations were performed using a nonimmune goat serum, which verified the specificity of the bands detected by Western blotting using specific primary antibodies against to ERK1/2 (1:300) and Akt (1:300) (Santa Cruz Biotechnology, Inc).

Western blot analysis

The protein concentration from the total homogenate was measured using a Bio-Rad kit (Bio-Rad Protein Assay; Bio-Rad) and then thirty micrograms (30 μg) were run in 12% polyacrylamide gel (Sigma). To estimate the corresponding molecular weights, the Full Range Rainbow Molecular Weight Marker was used (Amersham). Proteins were transferred to a nitrocellulose membrane, and nonspecific binding was blocked with PBS containing 5% nonfat dried milk, 0.1% Tween 20 (blocking buffer) at room temperature. The membranes were then rinsed and incubated for 2 hours with the next appropriate primary antibodies: p-Smad2/3 goat polyclonal (1:300, C-terminal Ser423/425 residues), total ERK1 rabbit polyclonal (1:300), p-ERK1/2 goat polyclonal (1:300), Akt rabbit polyclonal antibody, p-Akt rabbit polyclona (1:300), TβRI rabbit polyclonal (1:300), β-actin mouse monoclonal antibody (1:700; Santa Cruz Biotechnology, Inc), or Smad4 rabbit polyclonal antibody (1:1000; Cell Signaling Technology). The blots were incubated with a peroxidase-conjugated (horseradish peroxidase) bovine antigoat (1:2500; Santa Cruz Biotechnology, Inc), goat-mouse (1:2500) or goat antirabbit secondary (1:2500; Thermo Scientific, Pierce Antibodies), diluted in a blocking buffer (1:5000). The membranes were thoroughly rinsed in PBS/0.1% Tween 20, and the horseradish peroxidase-coupled secondary antibody was revealed with enhanced chemiluminescence Western blotting detection reagents (GE Healthcare) following the manufacturer's instructions. Emitted light was captured on Hyperfilm (GE Healthcare), with signals being scanned and quantified with Scion Image software (version Beta 4.0.2; Scion Image Corp) at 3 different exposure times.

PRL determination

The PRL concentration in the culture medium was measured by a double-antibody RIA, with materials and protocols supplied by Dr A. F. Parlow from the National Hormone and Pituitary

Table 1. Details of Primary Antibodies Used in the Study

Peptide/Protein Target	Antigen Sequence (if known)	Name of Antibody	Manufacturer, Catalog Number, and/or Name of Individual Providing the Antibody	Species Raised in; Monoclonal or Polyclonal	Dilution Used
ERK1/2		ERK1/2 (K-23)	Santa Cruz Biotechnology, Inc, sc-94	Rabbit polyclonal IgG	1:300
Akt		Akt 1/2/3 (H136)	Santa Cruz Biotechnology, Inc, sc-8312	Rabbit polyclona IgG	1/300
p-ERK		p-ERK1/2	Santa Cruz Biotechnology, Inc, sc-16982	Goat polyclonal IgG	1:300
p-Akt		p-Akt 1/2/3 (Ser473)-R	Santa Cruz Biotechnology, Inc, sc-33437-R	Rabbit polyclona IgG	1:300
p-Smad2/3		p-Smad2/3 (C-terminal Ser423/425 residues)	Santa Cruz Biotechnology, Inc, sc-11769	Goat polyclonal IgG	1:300
Smad4		Smad4	Cell Signaling Technology, 9515	Rabbit polyclona	1:1000
TGFβRI		TGFβRI (V-22)	Santa Cruz Biotechnology, Inc, sc-398	Rabbit polyclona IgG	1:300
Actin		Actin (H-6)	Santa Cruz Biotechnology, Inc, sc-376421	Mouse monoclonal IgG	1:700
Bromodeoxyuridine		Bromodeoxyuridine (clone BU-1)	GE Healthcare Life Sciences, RPN 202	Monoclonal antimouse	1:100

Program. The assay sensitivity was 1-ng/mL medium, and the interand intraassay coefficients of variation were 10%.

Confocal laser scanning microscopy

Pituitary cells were fixed in 4% formaldehyde, permeabilized in 0.25% Triton X-100 in PBS, blocked for 1 hour in 3% PBS-BSA, and incubated with the next primary antibodies: p-Smad2/3 goat polyoclonal (1:300) and p-Akt rabbit polyclonal antibody (1:300) or p-ERK 1/2 goat polyclonal (1:300; Santa Cruz Biotechnology, Inc) for 1 hour. The coverslips were washed with PBS and incubated with anti-BrdU (GE Healthcare) for 1 hour. Then, these cells were washed and further incubated with an Alexa Fluor 488 antigoat, Alexa Fluor 594 antirabbit, or Alexa Fluor 594 antimouse secondary antibody (1:1000; Invitrogen) for 1 hour. Images were then obtained using an inverted confocal laser scanning microscope FluoView FV 1000 (Olympus). An Ar-ion 488-nm laser was used for excitation of green fluorescence and a 543 nm one for excitation of red fluorescence. Serial z-axis sections were collected with a ×60 or ×100 objective. The analysis of confocal microscopy images was carried out using FV10-ASW 1.6 Viewer software.

Colocalization measurements in confocal images

To assess the extent of colocalization between p-Smad2/3 and ERK1/2 and between p-Smad2/3 and Akt, the tiff images acquired with confocal laser scanning microscope FluoView FV 1000 (Olympus) were processed in Adobe Photoshop for presentation. For colocalization measurements, raw unprocessed images were opened with ImageJ 1.46r (National Institutes of Health). These images were converted to an 8 bit gray scale, and the "Colocalization Finder" plug-in algorithm was used to generate the Pearson's coefficient per dual channel image in order to indicate the degree of colocalization.

Immunogold electron microscopy (EM)

The subcellular localization of p-Smad2/3, ERK1/2, and Akt in the GH3B6 cells was examined by an ultrastructural immunocytochemical technique applying protocols previously standardized in our laboratory (24). Thin sections were cut using a JEOL ultramicrotome with a diamond knife. Grids were incubated with the next antibodies: p-Smad2/3 goat polyclonal (1:300), ERK1/2 rabbit polyclonal (1:300), Akt rabbit polyclonal (1:300; Santa Cruz Biotechnology, Inc) or Smad4 rabbit polyclonal (1:1000; Cell Signaling Technology) overnight at 4°C. The sections were washed with PBS and incubated with antigoat and antirabbit secondary antibodies conjugated to 15 nm (Electron Microscopy Sciences) or 5 nm (Sigma-Aldrich) colloidal gold particles, respectively, diluted 1:30 in 1% PBS-BSA. To validate the specificity of the immunostaining, the next controls were performed: 1) replacement of primary antiserum with 1% BSA in PBS; and 2) replacement of primary antiserum with diluted preimmune serum followed by the secondary antibody. Then, sections were examined in a Zeiss LEO 906-E transmission EM (TEM) and photographed with a megaview III camera.

Statistical analysis

Experimental points represent the mean ± SEM of 3 replicates measured in 3 independent cell cultures. Statistical analysis was carried out using ANOVA, followed by the Fisher test using the InfoStat program. Significance levels were chosen as $P < .05$ for the Fisher test.

Results

Inhibition of MEK and PI3K potentiates the antimitogenic effect of TGFβ1 in GH3B6 cells

In order to determine the effect of TGFβ1 treatment on the proliferation of GH3B6 pituitary tumor cells, the cells were incubated with different doses of this cytokine (2 or 4 ng/mL), as well as using different exposure times (7, 16, and 24 h) in culture medium with serum, revealing that the antimitogenic effect of TGFβ1 was dose and time dependent (see Supplemental Figure 1). Therefore, considering that the most significant results were observed with the dose of 4 ng/mL and 24 hours of treatment, we selected these experimental conditions for the protocols. As shown in Figure 1A, TGFβ1 treatment induced an increase of cells in the G_0/G_1 phase ($P < .05$), with a corresponding reduction in the number of cells in the proliferative fraction ($S + G_2/M$) ($P < .05$). In parallel, we evaluated whether TGFβ1 induced apoptosis in GH3B6 tumoral pituitary cells using transferase (TdT)-mediated dUTP nick-end labeling and Annexin V-fluorescein isothiocyanate/propidium iodide (PI) staining assays. The percentage of apoptosis in GH3B6 treated with TGFβ1 for 24 hours did not change with respect to control cells (see Supplemental Materials and Methods and Supplemental Figure 2, A and B). For our experimental conditions, we demonstrated that GH3B6 cells were sensitive to TGFβ1-induced cell cycle arrest but were unable to elicit an apoptosis response.

To investigate whether the MEK/ERK and PI3K/Akt pathways could regulate TGFβ1-induced cell cycle arrest, we analyzed cell cycle progression by using MEK (PD98059) and PI3K (LY294002) inhibitors before TGFβ1 stimulus. As shown in Figure 1A, TGFβ1 treatment induced an increase of cells in the G_0/G_1 phase ($P < .05$), with a corresponding reduction in the number of cells in the proliferative fraction ($S + G_2/M$) ($P < .05$). The inhibitors of MEK and PI3K enhanced the antiproliferative response of TGFβ1, which was evidenced by a further increase in the number of cells in the G_0/G_1 phase and by a reduction in the number of cells in the S and G_2/M phases ($P < .05$). In addition, we quantified the ability to incorporate BrdU as a measure of entry into the S phase of the cell cycle after TGFβ1 treatment in the presence of PD98059 or LY294002. As shown in Figure 1B, the bivariated PI-BrdU flow cytometry was in agreement with the results of the cell cycle, demonstrating that both inhibitors potentiated the antiproliferative effect of TGFβ1.

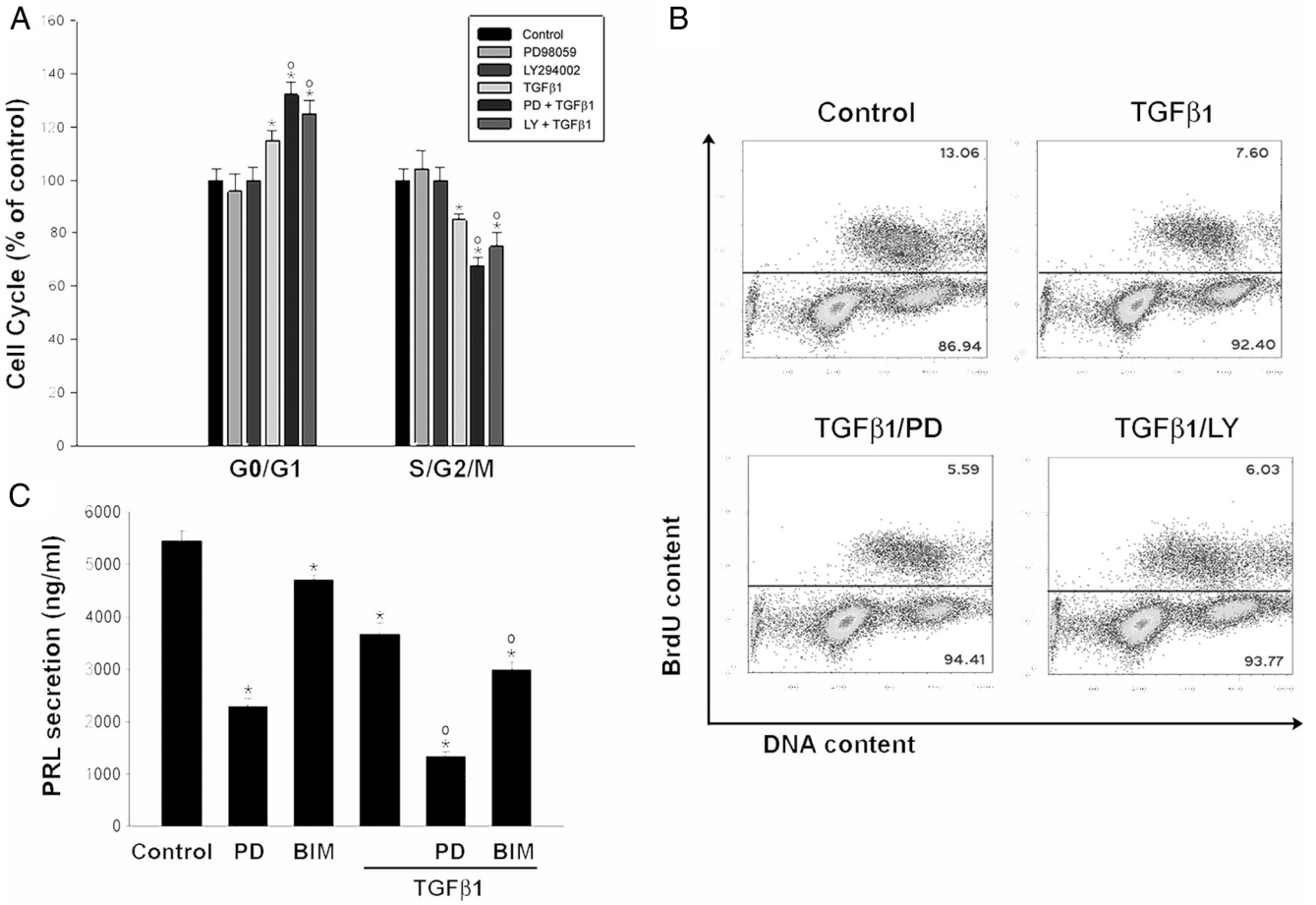

Figure 1. Effect of TGFβ1 on GH3B6 cell proliferation. After pretreatment with PD98059 (PD) (50μM) or LY294002 (LY) (10μM) for 30 minutes, GH3B6 cells were treated with TGFβ1 (4 ng/mL) for 24 hours. A, Cells were collected, stained with propidium iodide, and analyzed for cell cycle distribution using flow cytometry. The percentage of cells in the proliferative fraction (S + G_2/M) is expressed relative to the control cells (the control data were set to 100%). The data are represented as mean ± SD of 3 independent experiments. *, $P < .05$ vs control; 0, $P < .05$ vs TGFβ1. B, Flow cytometric analysis after TGF-β1 treatment in the presence or absence of PD or LY inhibitors, employing BrdU staining and PI counterstaining. The percentage of BrdU-staining cells at each experimental condition is indicated. The image corresponds to a representative experiment from a total of 3 with similar results. C, Effect of TGFβ1 and PKCs/MEK/ERK1/2 pathways on PRL release. GH3B6 cells were pretreated with PD98059 (50μM) or BIM (4μM) for 30 minutes and then stimulated with TGFβ1 (4 ng/mL) for 24 hours. The data are expressed as the mean ± SD from 5 independent experiments. *, $P < .01$ vs control; 0, $P < .01$ vs TGFβ1.

These experiments led us to propose that MEK and PI3K could be key modulators of the antimitogenic effect of TGFβ1 in GH3B6 cells.

PKC and MEK inhibitors coincubated with TGFβ1 induced an additive inhibitor effect on PRL release

Considering our previous reports that have demonstrated the participation of PKCs and ERK1/2 in prolactin release in normal pituitary cells in response to different stimuli (25, 26), here we attempted to characterize the influence of the PKC/MEK/ERK pathway on the TGFβ1-induced PRL release effect. Under baseline conditions, the significant reduction in PRL levels detected after incubation with both inhibitors ($P < .01$) supported the contribution of PKCs/MEK/ERK1/2 pathways in regulating the constitutive PRL release from GH3B6 tumoral pituitary cells (Figure 1C). The treatment with TGFβ1 for 24 hours significantly inhibited PRL release ($P < .01$), with an additive inhibitory effect on PRL release being observed when the cells were incubated with TGFβ1 in the presence of the MEK or BIM inhibitors, thereby indicating the contribution of both pathways to this effect.

The activation of Smad2/3 induced by TGFβ1 was regulated by PI3K and ERK1/2

Considering that the receptor-mediated phosphorylation of Smads can be regulated by the MEK/ERK and PI3K/Akt pathways, we examined the Smad2/3 activation induced by TGFβ1 in the presence of PD98059 or LY294002 (Figure 2A). By Western blotting, it was shown that a greater increase in p-Smad2/3 expression occurred when TGFβ1-treated GH3B6 cells were preincubated with MEK or PI3K inhibitors ($P < .05$), suggesting that the activation of the canonical signal TGFβ1/Smad2/3 was

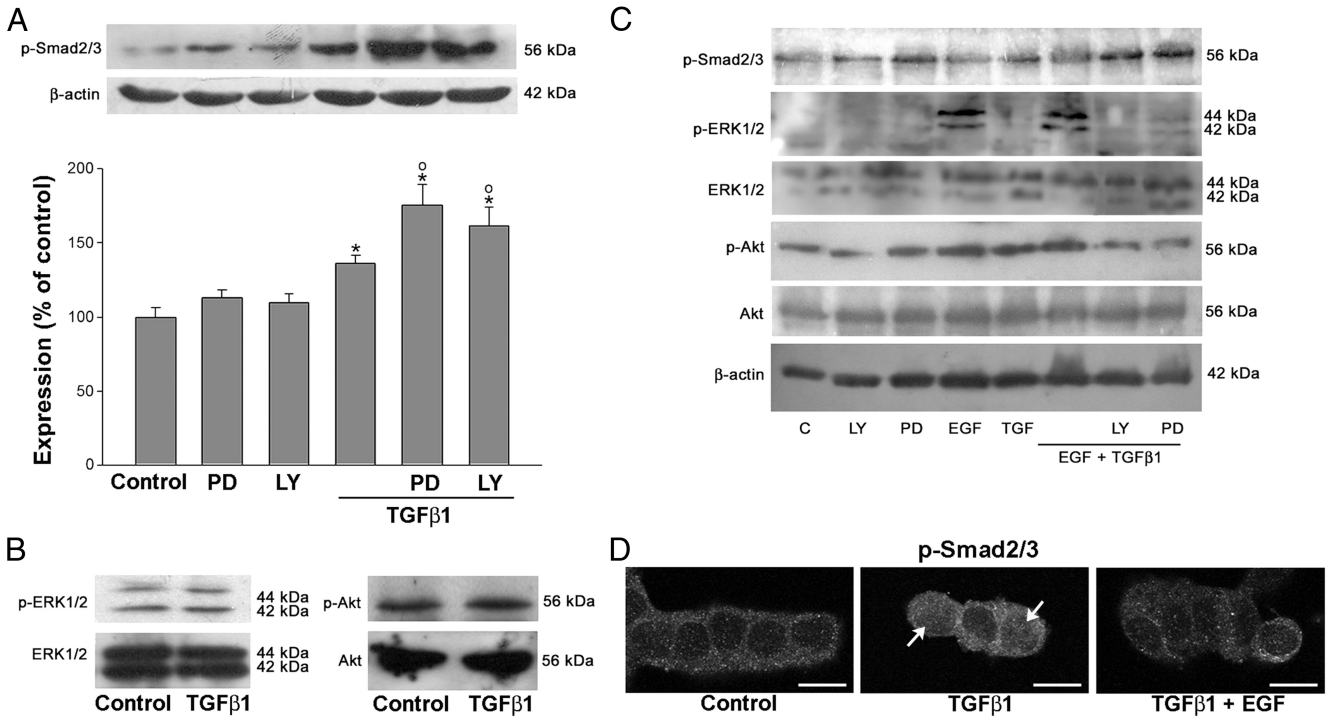

Figure 2. MEK and PI3K modulated the activation of Smad2/3 induced by TGFβ1. A, The GH3B6 cells were treated with TGFβ1 (4 ng/mL) for 30 minutes in the presence of PD98059 (PD) (50μM) and LY294002 (LY) (10μM), and the endogenous p-Smad2/3 was analyzed by Western blotting. The p-Smad2/3-β-actin ratio is represented as a percentage relative to the untreated control (control data were set to 100%). The data are expressed as mean ± SD of 3 independent experiments. *, $P < .01$ vs control; 0, $P < .01$ vs TGFβ1. B, Effect of TGFβ1 on ERK1/2 and Akt activation. The image corresponds to a representative experiment from a total of 3 with similar results. C, EGF activates ERK1/2 and Akt, which inhibits the phosphorylation of Smad2/3 induced by TGFβ1. The cells were coincubated with EGF and TGFβ1 in the presence or absence of PD or LY inhibitors. The image corresponds to a representative experiment from a total of 3 with similar results. D, The GH3B6 cells were treated with TGFβ1 for 30 minutes in the presence or absence of EGF and were then analyzed by confocal microscopy. TGFβ1 induced nuclear accumulation of p-Smad2/3 (arrows), effect that was attenuated by the coincubation with EGF. Scale bar, 20 μm.

inhibited by the MEK/ERK and PI3K/Akt pathways. To evaluate whether TGFβ1 induces ERK1/2 and Akt activation, the GH3B6 cells were treated with TGFβ1 for 30 minutes, and their phosphorylated states were determined by Western blotting. In Figure 2B, it can be observed that the analysis of the p-ERK1/2 and p-Akt signals revealed no changes in the ERK1/2 or PI3K/Akt pathway activation after TGFβ1 stimulation. In agreement with these results, in anterior pituitary cells, it has been reported that short exposition to TGFβ1 was unable to activate the ERK1/2 signaling pathway (27).

Taking into account that the MEK/ERK and PI3K/Akt pathways can be activated by the EGF (28), we investigated the ability of EGF to regulate the TGFβ/Smad signaling by activating the MEK/ERK and PI3K/Akt pathways. As shown in Figure 2C, the EGF treatment alone did not alter the levels of p-Smad2/3 compared with the control. However, coincubation with TGFβ1 decreased the expression compared with TGFβ1 alone. This effect of EGF on the TGFβ1-induced p-Smad2/3 activation was reverted when the cells were treated with both growth factors in the presence of MEK or PI3K inhibitors. In addition, we analyzed the p-ERK and p-Akt expression in the total extract and observed that the levels of both kinases were inversely related to the p-Smad2/3 expression visualized for these experimental conditions.

Next, we examined the effect of EGF on the TGFβ1-induced nuclear accumulation of Smad2/3 by confocal microscopy. In the absence of growth factor stimulation, p-Smad2/3 was predominantly cytoplasmatic (Figure 2D). The TGFβ1 treatment induced nuclear accumulation of p-Smad2/3, an effect that was attenuated when the cells were incubated with TGFβ1 in the presence of EGF.

These observations can be interpreted as a counterbalancing mechanism, where the proliferative stimulation of EGF, which activates the ERK1/2 and Akt pathways, modulates the Smad2/3 phosphorylation and nuclear translocation induced by TGFβ1.

ERK1/2 and Akt interact with Smad2/3 in GH3B6 cells

The next step was to investigate the possible interactions of Smad2/3 with ERK1/2 or Akt using immunopre-

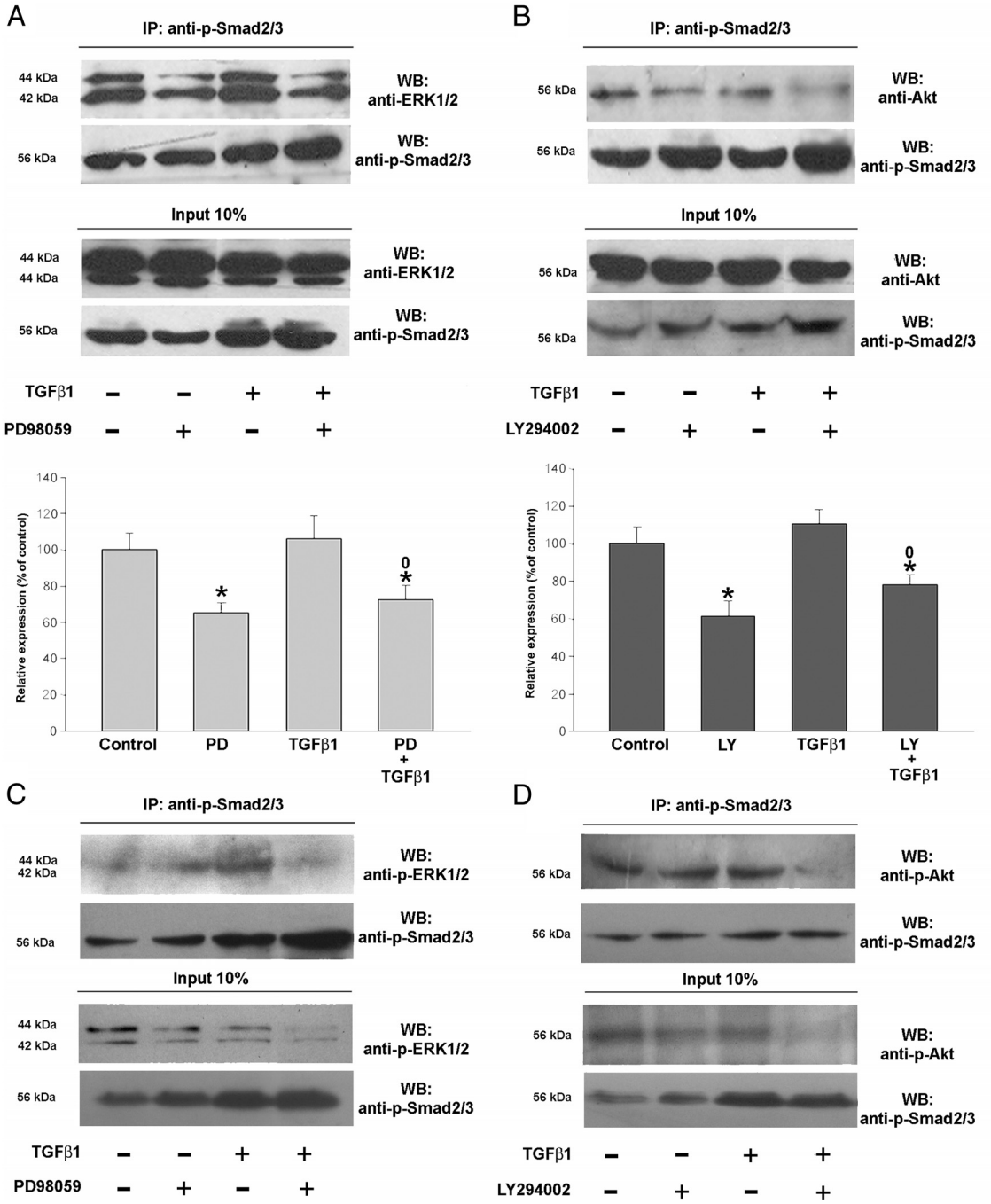

Figure 3. Interaction of Smad2/3 with ERK1/2 or Akt. GH3B6 cells were treated with TGFβ1 (4 ng/mL) for 30 minutes after preincubation with PD98059 (PD) (50μM) and LY294002 (LY) (10μM) for 30 minutes. Cell lysates were immunoprecipitated with Protein G-Sepharose in combination with the anti-p-Smad2/3 primary antibody. The immunoprecipitated fractions and the whole lysates were analyzed by Western blotting using the next antibodies: anti-ERK1/2 (A) anti-Akt (B), anti-p-ERK1/2 (C), or anti-p-Akt (D). One experiment representative of 3 independent ones with similar results is shown. The IP p-Smad2/3-ERK1/2 or IP p-Smad2/3-Akt expression index is represented as a percentage relative to the untreated control (control data were set to 100%). The data are expressed as mean ± SD of 3 independent experiments. *, $P < .01$ vs control; 0, $P < .01$ vs TGFβ1.

cipitation studies on GH3B6 cells treated with TGFβ1 in the presence of PD98059 or LY294002 inhibitors.

In Figure 3, A and B, a baseline interaction can be observed between p-Smad2/3 and ERK1/2 or Akt, which decreased after incubation with the MEK or PI3K inhibitors ($P < .05$), respectively, indicating that an activated state of ERK1/2 or Akt may be necessary for the existence of these interactions. When the GH3B6 cells were incubated with TGFβ1 for 30 minutes in the presence of the PD989059 or LY294002 inhibitors, the interaction of p-Smad2/3-ERK1/2 or p-Smad2/3-Akt decreased compared with the treatment with TGFβ1 alone ($P < .05$). To

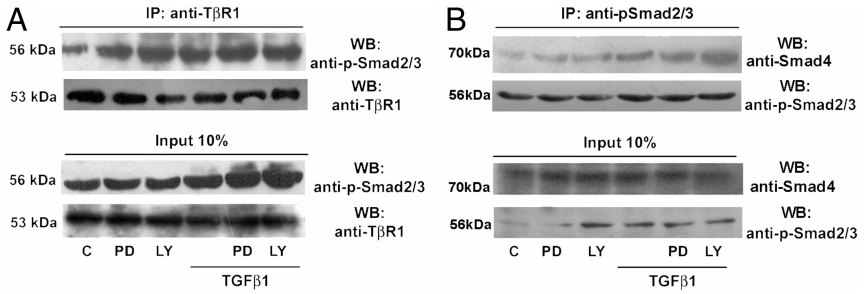

Figure 4. The ERK1/2 and Akt activation modulated the association of Smad2/3 with TβRI (A) or Smad4 (B). These interactions were analyzed by immunoprecipitation in the GH3B6 cells treated with TGFβ1 in the presence of the MEK (PD) or PI3K (LY) inhibitors. The images correspond to a representative experiment from a total of 3 with similar results.

try to confirm whether the activated state of ERK1/2 or Akt interacts with p-Smad2/3, immunoprecipitation assays using p-ERK1/2 and p-Akt were performed. As shown in Figure 3, C and D, a low baseline interaction can be observed between p-Smad2/3 and p-ERK1/2 or p-Akt, which increased after treatment with TGFβ1 for 30 minutes, with these effects being reverted by preincubation with the MEK or PI3K inhibitors, thus indicating that an phosphorylated state of ERK1/2 or Akt may be necessary for the existence of these interactions.

MEK and PI3K inhibitors increase the interaction of Smad2/3 with TβRI or Smad4

A possible mechanism to regulate Smad2/3 phosphorylation is by controlling the pool of Smad2/3 available for TGFβ signaling. The high phosphorylation of Smad2/3 in the presence of PI3K and MEK inhibitors (Figure 2A) and the interaction between Smad2/3 with ERK1/2 or Akt (Figure 3) led us to hypothesize that both kinases altered the Smad2/3 phosphorylation induced by TβRI. To evaluate this, we analyzed the interaction of Smad2/3 with TβRI by immunoprecipitation in the GH3B6 cells treated with TGFβ1 in the presence of the MEK or PI3K inhibitors. As shown in Figure 4A, both inhibitors increased the interaction between Smad2/3 and TβRI, suggesting that the activation of ERK1/2 and Akt may have inhibited Smad2/3 phosphorylation by interfering with its association with the TGFβ receptor.

In order to determine whether the interaction of p-Smad2/3 with Smad4 was affected by the MEK/ERK and PI3K/Akt pathways, we performed immunoprecipitation experiments in TGFβ1-treated cells with or without PD98059 or LY294002 inhibitors. As shown the Figure 4B, both inhibitors increased the interaction between Smad2/3 and Smad4, suggesting that the activation of ERK1/2 and Akt may have regulated the TGFβ1 signaling by modulating the association of Smad2/3 with Smad4.

Subcellular localization of Smad2/3, ERK1/2, and Akt in GH3B6 cells

Confocal microscopy

The subcellular localization of Smad2/3, ERK, and Akt is closely associated with their activation and functions. Thus, we analyzed the intracellular distribution and colocalization of these kinases in basal and TGFβ1-treated conditions using confocal microscopy. In control GH3B6 cells, the immunofluorescence of p-Smad2/3 was mainly cytoplasmic (Figure 5, A and B). However, after TGFβ1 stimulus, a greater immunolabeled p-Smad2/3 in the nucleus and near to the plasma membrane was detected, which might be indicative of their activated states.

The colocalization of p-Smad2/3 with p-ERK1/2 or p-Akt was visualized in basal and TGFβ1-treated conditions. This was confirm using ImageJ software to calculate the Pearson's coefficient (see experimental procedures in colocalization measurements), which indicated that there had indeed been colocalization between p-Smad2/3-ERK and p-Smad2/3-Akt (Figure 5C).

Immuno-EM

To investigate further the results obtained by confocal microscopy, we analyzed the fine localization of p-Smad2/3 with ERK1/2 or Akt by means of TEM immunogold labeling in control and TGFβ1-treated tumoral lactosomatotroph cells. Under both conditions, the immunoreactivities for p-Smad2/3 with ERK1/2 or Akt were distributed throughout the cytoplasm and were occasionally observed at the plasma membrane and nucleus compartment (Figures 6 and 7).

Concerning the association observed by TEM, the gold particles identifying p-Smad2/3 with ERK or Akt (~5 nm) were observed to be close to each other, thus suggesting a physical interaction. To investigate this special proximity between the 2 enzymes, Smad2/3 and Smad4 were used as positive controls, with this complex being visualized in the cytoplasm and nucleus in basal and treated TGFβ1 conditions. As shown in Figure 7C, the distance between the gold particles for p-Smad2/3 and Smad4 was similar to that obtained for p-Smad2/3 with ERK1/2 or Akt.

Discussion

In the present study, we demonstrated that the antimitogenic effect of TGFβ1 in GH3B6 pituitary tumor cells was

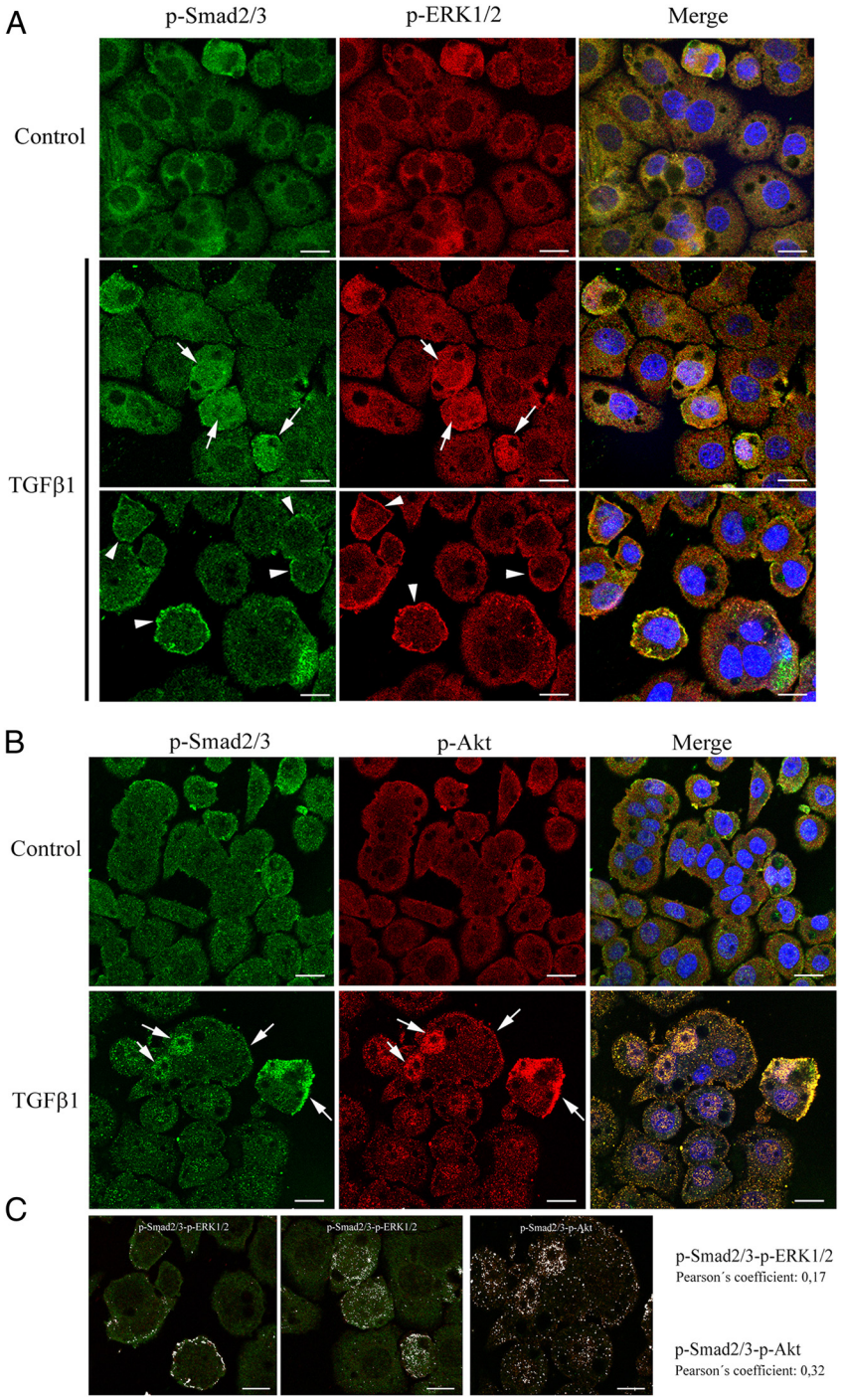

Figure 5. Colocalization of p-Smad2/3 with p-ERK1/2 or p-Akt. The intracellular localization of p-Smad2/3, p-ERK1/2, and p-Akt were analyzed by confocal laser scanning microscopy in control and TGFβ1-treated GH3B6 cells. The TGFβ1 (4 ng/mL) stimulus for 30 minutes induced a notable p-Smad2/3 translocation from the cytoplasm to the nucleus and plasma membrane (arrows). p-ERK1/2 (A) and p-Akt (B) immunostaining showed a similar subcellular localization compared with the p-Smad2/3 after the treatment with TGFβ1. C, TGFβ1-treated GH3B6 cells labeled with anti-p-Smad2/3 and p-ERK1/2 or p-Akt. p-Smad2/3 and p-ERK1/2 colocalize in cytoplasm, nucleus, and plasma membrane as shown by the white dots obtained after the image processing with ImageJ software using the Colocalization Finder plug-in. Colocalization of p-Smad2/3 with p-Akt is similar to p-Smad2/3-p-ERK1/2 observing white dots in cytoplasm, nucleus, and plasma membrane. The right panel shows the Pearson's coefficient generated by the Colocalization Finder plug-in. Scale bar, 10 μm.

modulated by the MEK/ERK1/2 and PI3K/Akt pathways. Treatment with TGFβ1 caused an inhibition in the cell proliferation, with this being potentiated when the cells were preincubated with the MEK (PD98059) and PI3K (LY296002) inhibitors.

Evidence of cross talk between these 2 major signaling pathways responsible for regulating proliferation and the TGFβ1 pathways was observed in this study, suggesting that ERK1/2 and PI3K can counteract the antimitogenic effect of TGFβ1 in GH3B6 cells. Related to this, it has been previously reported that MEK/ERK and PI3K/Akt are both overexpressed and overactivated in pituitary adenomas (16, 17). Furthermore, we demonstrated that the PKC/MEK/ERK1/2 pathway stimulated cell cycle progression in GH3B6 cells (29). Thus, bearing in mind the proliferative role of the MAPK and PI3K pathways reported in tumoral pituitary cells, these constitutively activated pathways may in parallel inhibit the antimitogenic effect of TGFβ1, thereby explaining the low response to antiproliferative signals observed in GH3B6 cells. Although, prolactinomas are the most prevalent type of pituitary tumors in humans and generally respond well to medical therapy with dopamine agonists (30), in case of patients exhibiting resistance to dopaminergic drugs, alternative therapies are needed (31, 32). Recently, the synthetic thrombospondin 1 analogs have been proposed as potential alternatives or complementary treatments in dopamine agonist-resistant prolactinomas, because they improve TGFβ1 activity in pituitary tumors (33, 34). Therefore, the study of pituitary TGFβ1 regulation may provide novel tools that can be applied in alternative therapies to treat pituitary tumors.

It is well known that TGFβ1 synthesized in the pituitary may act as an

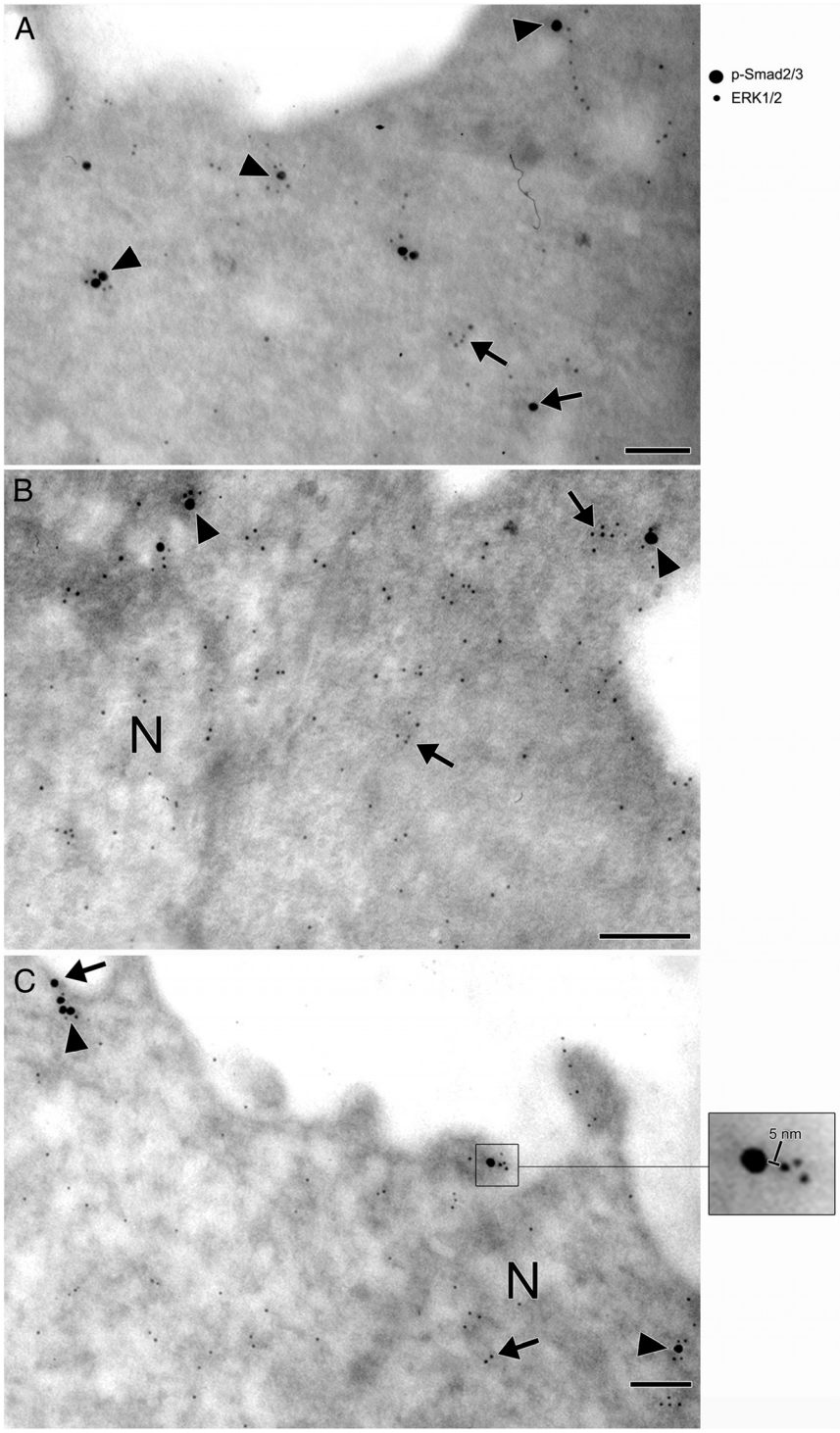

Figure 6. Immuno-EM for p-Smad2/3 and ERK1/2 in GH3B6 pituitary tumor cells. Three representative TEM images of the data obtained with immunogold labeling of p-Smad2/3 and ERK in GH3B6 cells treated with TGFβ1 (4 ng/mL) for 30 minutes. Two antibodies were used for generating each picture as indicated in the top right hand corner of micrograph. A–C, Localization of p-Smad2/3 (15-nm gold) and ERK1/2 (5-nm gold). Both proteins are found alone (arrows) or associated (arrowheads) in the cytoplasmic matrix and nucleus. C, High-magnification image (insets) is shown in the right of micrograph. The square box in the inset shows the special proximity (5 nm) between the 2 enzymes. Similar distance was observed (5 nm) between the gold particles identifying p-Smad2/3 with Smad4, which were used as positive control interaction (see Figure 8C). N, nucleus. Scale bar, 100 nm.

autocrine/paracrine regulator of the lactotroph function inhibiting the PRL secretion and PRL gene transcription (35). In the present study, we observed a significant decrease of PRL levels in culture medium after TGFβ1 alone, which was even more noticeable after BIM/TGFβ1 and PD98059/TGFβ1 coincubations. These results suggest that the activation of the TGFβ/Smads pathways and the inhibition of the PKC/MEK/ERK1/2 signal contributed to the PRL release inhibitor effect. These findings suggest the possibility of an improved effectiveness that could result from using an alternative therapy in resistant prolactinomas, which have previously failed to achieve normoprolactinemia or to induce tumor shrinkage after using dopamine agonists (31).

Having observed that the TGFβ1 signal is regulated by ERK1/2 and PI3K, we decided to investigate whether this modulation occurred at the level of Smad2/3 activation. Although Smads are activated by TβRI-mediated phosphorylation, their activity and stability are further regulated by downstream kinases of other signaling pathways (11). Here, we observed that the phosphorylation of Smad2/3 induced by TGFβ1 was enhanced when the cells were preincubated with the MEK and PI3K inhibitors, indicating a negative role of both pathways on the activation of Smad2/3. In addition, our results revealed phosphorylation of ERK1/2 and Akt by EGF, which blocked the TGFβ1 effect on Smad2/3 activation, thus reinforcing the idea of the existence of a counterbalancing mechanism in Smad2/3 regulation, defining a point of convergence between these mitogenic and antimitogenic signaling pathways. In agreement with this observation, it has been previously reported that EGF/

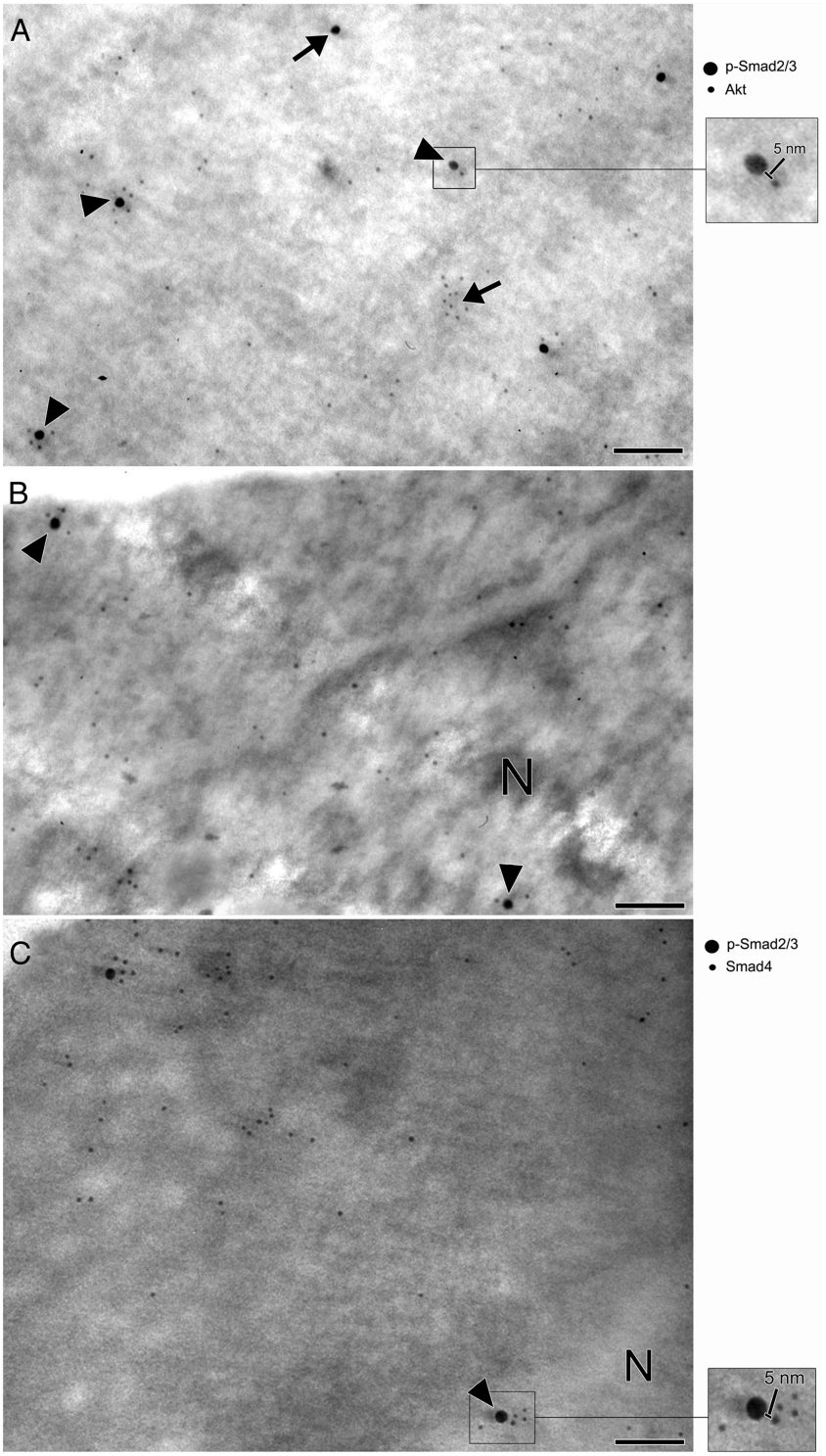

Figure 7. Immuno-EM for p-Smad2/3 and Akt in GH3B6 cells. Three representative TEM images of the data obtained with immunogold labeling of p-Smad2/3 and Akt in pituitary tumor cells treated with TGFβ1 (4 ng/mL) for 30 minutes. A and B, In treated cells, p-Smad2/3 (15-nm gold) and Akt (5-nm gold) immunoreactivities are distributed throughout cytoplasmic matrix and nucleus alone (arrows) or associated (arrowheads). High-magnification image (insets) is shown in the right of micrograph. The square box in the inset shows the special proximity (5 nm) between the p-Smad2/3 and Akt. C, Immuno-EM for p-Smad2/3 and Smad4. TGFβ1-treated GH3B6 cells show p-Smad2/3 (15 nm) and Smad4 (5 nm) immunogold labeling distributed in the cytoplasmic matrix and the nucleus alones (arrows) or associated (arrowheads). High-magnification image (insets) is shown in the right of micrograph. The square box in the inset illustrates the special proximity (5 nm) between the p-Smad2/3 and Smad4. N, nucleus. Scale bar, 100 nm.

MEK/ERK signaling specifically inhibits Smad3 activity (36).

In order to test the interaction between the downstream kinases of MEK and PI3K with Smad2/3, immunoprecipitation assays were performed, and an association of Smad2/3 with ERK1/2 or Akt was found under baseline conditions. Incubation with the MEK and PI3K inhibitors decreased this effect, indicating that the activated states of ERK1/2 and Akt were necessary in order to interact with Smad2/3. Moreover, these Smad2/3-ERK1/2 and Smad2/3-Akt associations were confirmed by confocal and TEM, where we observed the colocalization of Smad2/3 with ERK1/2 or Akt in the nucleus and plasma membrane of control and TGFβ1-treated cells.

Direct phosphorylation of Smad3 by MAPKs, such as ERK, JNK, and p38, has been previously demonstrated in different cell types, including normal lung and gastric cells and in breast cancer cells (37–39). Related to this, it has also been reported that the phosphorylation of Smad3 by MAPKs blocks the activation induced by TβRI (40, 41), which might explain, at least in part, our results referring to the greater phosphorylation in Smad2/3 promoted by TGFβ1 in the presence of the MEK inhibitor observed in GH3B6 cells. In addition, the counterbalanced regulation of TGFβ1/Smad2/3 by other signals might be one of the molecular mechanisms that contributes to the refractory response to the TGFβ1 effect.

Regarding the association between the Smad2/3 and the PI3K/Akt pathways, a direct interaction between Akt and Smad2 has been recently demonstrated in cultured human aortic endothelial cells (42). In fact, Akt may inhibit Smad3 by directly phosphorylating it or by physically sequestering Smad3 to prevent

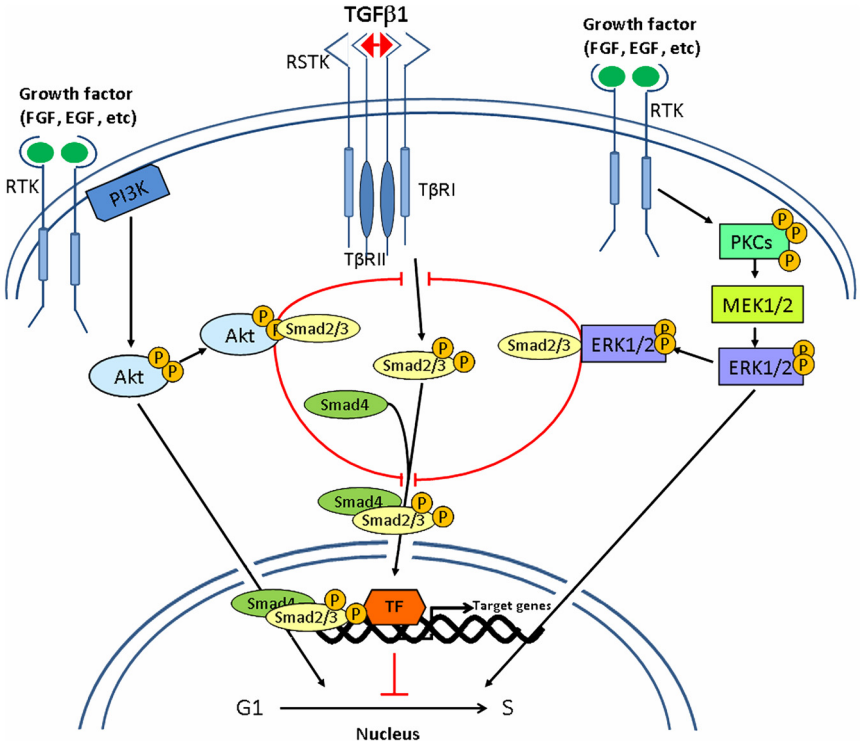

Figure 8. The next is the proposed model for the regulation of GH3B6 cell proliferation by cross talk of TGFβ1/Smad with MEK/ERK1/2 or PI3K/Akt pathways. The MEK/ERK1/2 and PI3K/Akt pathways impinge on TGFβ1/Smad2/3 signaling modulating Smad2/3 phosphorylation. The direct associations of ERK1/2-Smad2/3 and Akt-Smad2/3 inhibit the TβRI induced-Smad2/3 activation counteracting the antimitogenic effect of TGFβ1. Also, ERK1/2 and Akt act by modulating the Smad2/3-Smad4 complex. Both mechanisms could be involved in the refractory behavior of GH3B6 pituitary tumor cells to the inhibitory effect of TGFβ1. Receptor tyrosine linase (RTK), receptor serine threonine kinase (RSTK), transcription factor (TF).

its activation. In 293T cells, it was previously demonstrated that, in the presence of serum, activated Akt formed a higher affinity complex with Smad3, resulting in the sequestration of Smad3 outside the nucleus and preventing its activation (43). This mechanism, which controls the pool of Smad2/3 available for TGFβ signaling, may regulate the phosphorylation induced by TβRI. In the present study, we observed that the interaction between Smad2/3 and TβRI was enhanced in the presence of MEK or PI3K inhibitors.

It is known that the phosphorylation of Smad2/3 is facilitated by physical interactions between the positively charged L3 loop region in Smad2/3 and the L45 loop and GS region of the receptor TβRI (44–46). Considering our results, which described a direct physical interaction between Smad2/3 and ERK1/2 or Akt observed by immunoprecipitation and confocal microscopy and EM, the MEK/ERK1/2 and PI3K/Akt pathways may regulate the TGFβ1 signaling in tumoral pituitary cells by physically sequestering Smad2/3 and/or by directly phosphorylating the concensus sites of ERK1/2 and Akt in L3 loop region of Smad2/3 that might alter the activation by TβRI. In addition, we observed that the activation of ERK1/2 and Akt can modulate the association of Smad2/3 with Smad4 and consequently the TGFβ1 signaling in tumoral pituitary cells. This regulatory mechanism exerted by ERK1/2 and Akt may occur at 2 levels: by interfering with the association of Smad2/3 with the TGFβ receptor I, which is indispensable for phosphorylation of Smad2/3, and by affecting the Smad2/3-Smad4 interaction, which is necessary for the regulation of TGFβ1 target genes.

In conclusion, in the present study, we have demonstrated that the antimitogenic effect of TGFβ1 in GH3B6 pituitary tumor cells is counterbalanced by the MEK/ERK1/2 and PI3K/Akt pathways via modulation of the Smad2/3 phosphorylation, in addition to the described proliferative effect that mediates these kinases (Figure 8). Furthermore, the high expression of ERK1/2 and PI3K detected in tumoral pituitary cells may have been responsible, at least in part, for the limited antiproliferative response to TGFβ1. Future studies to determine the participation of the intracellular mediators that regulate the antimitogenic signals will be key to understanding why pituitary tumor cells are refractory to the inhibitory effect of TGFβ1 and also to identify the kinases involved in adenohypophyseal disorders.

Acknowledgments

We thank PhD Marta Soaje for PRL-RIA assays, Mrs Elena Pereyra for her excellent technical assistance in TEM, and native speaker Dr Paul Hobson for revising the English of the manuscript. M.E.S. and A.M.B. are doctoral fellows at Consejo Nacional de Investigaciones Científicas y Técnicas and Fondo Nacional de Ciencia y Tecnología respectively. L.d.V.S. is a postdoctoral fellow at Consejo Nacional de Investigaciones Científicas y Técnicas. J.P.P, S.G., A.L.D.P., and A.I.T. are established researchers at Centro de Microscopía Electrónica, Instituto de Investigaciones en Ciencias de la Salud, Consejo Nacional de Investigaciones Científicas y Técnicas, Facultad de Ciencias Médicas, Universidad Nacional de Córdoba.

Address all correspondence and requests for reprints to: Juan Pablo Petiti, PhD, Centro de Microscopía Electrónica, Instituto

de Investigaciones en Ciencias de la Salud-Consejo Nacional de Investigaciones Científicas y Técnicas, Facultad de Ciencias Médicas, Universidad Nacional de Córdoba, Haya de la Torre y Enrique Barros, 5000-Córdoba, Argentina. E-mail: jpetiti@cmefcm.uncor.edu.

This work was supported by Fondo Nacional de Ciencia y Tecnología, Consejo Nacional de Investigaciones Científicas y Técnicas and Secretaría de Ciencia y Tecnología de la Universidad Nacional de Córdoba.

Disclosure Summary: The authors have nothing to disclose.

References

1. **Hentges S, Sarkar DK.** Transforming growth factor-β regulation of estradiol-induced prolactinomas. *Front Neuroendocrinol*. 2001;22:340–363.
2. **Mishra L, Derynck R, Mishra B.** Transforming growth factor-β signaling in stem cells and cancer. *Science*. 2005;310:68–71.
3. **Derynck R, Akhurst RJ, Balmain A.** TGF-β signaling in tumor suppression and cancer progression. *Nat Genet*. 2001;29:117–129.
4. **Minami S, Sarkar DK.** Transforming growth factor-β 1 inhibits prolactin secretion and lactotropic cell proliferation in the pituitary of oestrogen-treated Fischer 344 rats. *Neurochem Int*. 1997;30:499–506.
5. **Hentges S, Pastorcic M, De A, Boyadjieva N, Sarkar DK.** Opposing actions of two transforming growth factor-β isoforms on pituitary lactotropic cell proliferation. *Endocrinology*. 2000;141:1528–1535.
6. **Jin L, Tsumanuma I, Ruebel KH, Bayliss JM, Lloyd RV.** Analysis of homogeneous populations of anterior pituitary folliculostellate cells by laser capture microdissection and reverse transcription-polymerase chain reaction. *Endocrinology*. 2001;142:1703–1709.
7. **Sarkar DK, Pastorcic M, De A, Engel M, Moses H, Ghasemzadeh MB.** Role of transforming growth factor (TGF)-β type I and TGF-β type II receptors in the TGF-β1-regulated gene expression in pituitary prolactin-secreting lactotropes. *Endocrinology*. 1998;139:3620–3628.
8. **Pastorcic M, De A, Boyadjieva N, Vale W, Sarkar DK.** Reduction in the expression and action of transforming growth factor β 1 on lactotropes during estrogen-induced tumorigenesis in the anterior pituitary. *Cancer Res*. 1995;55:4892–4898.
9. **Kang JS, Liu C, Derynck R.** New regulatory mechanisms of TGF-β receptor function. *Trends Cell Biol*. 2009;19:385–394.
10. **Mu Y, Gudey SK, Landström M.** Non-Smad signaling pathways. *Cell Tissue Res*. 2012;347:11–20.
11. **Matsuzaki K.** Smad phosphoisoform signaling specificity: the right place at the right time. *Carcinogenesis*. 2011;32:1578–1588.
12. **Chen RH, Chang MC, Su YH, Tsai YT, Kuo ML.** Interleukin-6 inhibits transforming growth factor-β-induced apoptosis through the phosphatidylinositol 3-kinase/Akt and signal transducers and activators of transcription 3 pathways. *J Biol Chem*. 1999;274:23013–23019.
13. **Song K, Cornelius SC, Reiss M, Danielpour D.** Insulin-like growth factor-I inhibits transcriptional responses of transforming growth factor-β by phosphatidylinositol 3-kinase/Akt-dependent suppression of the activation of Smad3 but not Smad2. *J Biol Chem*. 2003;278:38342–38351.
14. **Nicolás FJ, Hill CS.** Attenuation of the TGF-β-Smad signaling pathway in pancreatic tumor cells confers resistance to TGF-β-induced growth arrest. *Oncogene*. 2003;22:3698–3711.
15. **McCubrey JA, Steelman LS, Chappell WH, et al.** Roles of the Raf/MEK/ERK pathway in cell growth, malignant transformation and drug resistance. *Biochim Biophys Acta*. 2007;1773:1263–1284.
16. **Cakir M, Grossman AB.** Targeting MAPK (Ras/ERK) and PI3K/Akt pathways in pituitary tumorigenesis. *Expert Opin Ther Targets*. 2009;13:1121–1134.
17. **Dworakowska D, Wlodek E, Leontiou CA, et al.** Activation of RAF/MEK/ERK and PI3K/AKT/mTOR pathways in pituitary adenomas and their effects on downstream effectors. *Endocr Relat Cancer*. 2009;16:1329–1338.
18. **McIntyre DJ, Robinson SP, Howe FA, et al.** Single dose of the antivascular agent, ZD6126 (N-acetylcolchinol-O-phosphate), reduces perfusion for at least 96 hours in the GH3 prolactinoma rat tumor model. *Neoplasia*. 2004;6:150–157.
19. **Rodrigues LM, Maxwell RJ, McSheehy PM, et al.** In vivo detection of ifosfamide by 31P-MRS in rat tumours: increased uptake and cytotoxicity induced by carbogen breathing in GH3 prolactinomas. *Br J Cancer*. 1997;75:62–68.
20. **Alessi DR, Cuenda A, Cohen P, Dudley DT, Saltiel AR.** PD 098059 is a specific inhibitor of the activation of mitogen-activated protein kinase kinase in vitro and in vivo. *J Biol Chem*. 1995;270:27489–27494.
21. **Sosa Ld, Gutiérrez S, Petiti JP, et al.** 17β-Estradiol modulates the prolactin secretion induced by TRH through membrane estrogen receptors via PI3K/Akt in female rat anterior pituitary cell culture. *Am J Physiol Endocrinol Metab*. 2012;302:E1189–E1197.
22. **Hussaini IM, Trotter C, Zhao Y, et al.** Matrix metalloproteinase-9 is differentially expressed in nonfunctioning invasive and noninvasive pituitary adenomas and increases invasion in human pituitary adenoma cell line. *Am J Pathol*. 2007;170:356–365.
23. **Terry NH, White RA.** Flow cytometry after bromodeoxyuridine labeling to measure S and G2+M phase durations plus doubling times in vitro and in vivo. *Nat Protoc*. 2006;1:859–869.
24. **Petiti JP, De Paul AL, Gutiérrez S, Palmeri CM, Mukdsi JH, Torres AI.** Activation of PKC ϵ induces lactotroph proliferation through ERK1/2 in response to phorbol ester. *Mol Cell Endocrinol*. 2008;289:77–84.
25. **Gutiérrez S, Petiti JP, De Paul AL, et al.** Antagonic effects of oestradiol in interaction with IGF-1 on proliferation of lactotroph cells in vitro. *Histochem Cell Biol*. 2005;124:291–301.
26. **De Paul AL, Gutierrez S, Sabatino ME, et al.** Epidermal growth factor induces a sexually dimorphic proliferative response of lactotroph cells through PKC/ERK1/2/Pit-1 in vitro. *Exp Physiol*. 2011;96:226–239.
27. **Coya R, Alvarez CV, Perez F, Gianzo C, Diéguez C.** Effects of TGF-β1 on prolactin synthesis and secretion: an in-vitro study. *J Neuroendocrinol*. 1999;11:351–360.
28. **Roskoski R Jr.** The ErbB/HER family of protein-tyrosine kinases and cancer. *Pharmacol Res*. 2014;79:34–74.
29. **Petiti JP, Gutiérrez S, De Paul AL, et al.** GH3B6 pituitary tumor cell proliferation is mediated by PKCα and PKCϵ via ERK 1/2-dependent pathway. *Cell Physiol Biochem*. 2010;26:135–146.
30. **Ciccarelli A, Daly AF, Beckers A.** The epidemiology of prolactinomas. *Pituitary*. 2005;8:3–6.
31. **Vasilev V, Daly AF, Vroonen L, Zacharieva S, Beckers A.** Resistant prolactinomas. *J Endocrinol Invest*. 2011;34:312–316.
32. **Oh MC, Aghi MK.** Dopamine agonist-resistant prolactinomas. *J Neurosurg*. 2011;114:1369–1379.
33. **Recouvreux MV, Guida MC, Rifkin DB, Becu-Villalobos D, Díaz-Torga G.** Active and total transforming growth factor-β1 are differentially regulated by dopamine and estradiol in the pituitary. *Endocrinology*. 2011;152:2722–2730.
34. **Recouvreux MV, Camilletti MA, Rifkin DB, Becu-Villalobos D, Díaz-Torga G.** Thrombospondin-1 (TSP-1) analogs ABT-510 and ABT-898 inhibit prolactinoma growth and recover active pituitary transforming growth factor-β1 (TGF-β1). *Endocrinology*. 2012;153:3861–3871.
35. **Tan SK, Wang FF, Pu HF, Liu TC.** Differential effect of age on transforming growth factor-β 1 inhibition of prolactin gene expres-

sion versus secretion in rat anterior pituitary cells. *Endocrinology*. 1997;138:878–885.
36. **Matsuura I, Wang G, He D, Liu F.** Identification and characterization of ERK MAP kinase phosphorylation sites in Smad3. *Biochemistry*. 2005;44:12546–12553.
37. **Kamaraju AK, Roberts AB.** Role of Rho/ROCK and p38 MAP kinase pathways in transforming growth factor-β-mediated Smad-dependent growth inhibition of human breast carcinoma cells in vivo. *J Biol Chem*. 2005;280:1024–1036.
38. **Kretzschmar M, Doody J, Timokhina I, Massagué J.** A mechanism of repression of TGFβ/Smad signaling by oncogenic Ras. *Genes Dev*. 1999;13:804–816.
39. **Mori S, Matsuzaki K, Yoshida K, et al.** TGF-β and HGF transmit the signals through JNK-dependent Smad2/3 phosphorylation at the linker regions. *Oncogene*. 2004;23:7416–7429.
40. **Ho J, Cocolakis E, Dumas VM, Posner BI, Laporte SA, Lebrun JJ.** The G protein-coupled receptor kinase-2 is a TGFβ-inducible antagonist of TGFβ signal transduction. *EMBO J*. 2005;24:3247–3258.
41. **Nagata H, Hatano E, Tada M, et al.** Inhibition of c-Jun NH2-terminal kinase switches Smad3 signaling from oncogenesis to tumor-suppression in rat hepatocellular carcinoma. *Hepatology*. 2009;49:1944–1953.
42. **Shepherd RD, Kos SM, Rinker KD.** Flow-dependent Smad2 phosphorylation and TGIF nuclear localization in human aortic endothelial cells. Am J Physiol Heart Circ Physiol. 2011;301:H98–H107.
43. **Conery AR, Cao Y, Thompson EA, Townsend CM Jr, Ko TC, Luo K.** Akt interacts directly with Smad3 to regulate the sensitivity to TGF-β induced apoptosis. *Nat Cell Biol*. 2004;6:366–372.
44. **Lo RS, Chen YG, Shi Y, Pavletich NP, Massagué J.** The L3 loop: a structural motif determining specific interactions between SMAD proteins and TGF-β receptors. *EMBO J*. 1998;17:996–1005.
45. **Feng XH, Derynck R.** A kinase subdomain of transforming growth factor-β (TGF-β) type I receptor determines the TGF-β intracellular signaling specificity. *EMBO J*. 1997;16:3912–3923.
46. **Wu JW, Hu M, Chai J, et al.** Crystal structure of a phosphorylated Smad2. Recognition of phosphoserine by the MH2 domain and insights on Smad function in TGF-β signaling. *Mol Cell*. 2001;8:1277–1289.